Measuring structural inhomogeneity of a helical conjugated polymer at high pressure and temperature

Tummas Napoleon Arge,[1] Zuzana Konôpková,[2] Dörthe Haase,[3] Hanns-Peter Liermann,[2] Ullrich Scherf,[4] Suchismita Guha,[5] Matti Knaapila[1]

[1]Department of Physics, Technical University of Denmark, 2800 Kgs. Lyngby, Denmark
[2]Photon Science DESY, 22607 Hamburg, Germany
[3]MAX IV Laboratory, Lund University, 22482 Lund, Sweden
[4]Macromolecular Chemistry Group (buwmacro), Bergische Universität Wuppertal, 42097 Wuppertal, Germany
[5]Department of Physics and Astronomy, University of Missouri, Columbia, MO 65211, USA
Correspondence to: S. Guha and M. Knaapila (E-mail: guhas@missouri.edu, matti.knaapila@fysik.dtu.dk)

ABSTRACT: We report on X-ray scattering measurements of helical poly[9,9-bis(2-ethylhexyl)-fluorene-2,7-diyl] by mapping the sample with 10 µm spatial resolution from 0.3 GPa to 36 GPa. We follow the strongest 00*l* reflection, which moves towards higher scattering angles with pressure indicating planarization of helical polyfluorene. Lateral inhomogeneity is increased for >10 GPa concomitant with the solidification of the pressure transmitting medium (a 4:1 mixture of methanol and ethanol). We also follow the 00*l* reflection with increasing temperature at the constant pressure of 4.3 GPa in neon. We observe a sharp shift towards higher scattering angles indicative of a phase transition at 167-176 °C.

KEYWORDS: polyfluorene; high pressure measurements

INTRODUCTION High pressure structural studies of π-conjugated polymers are motivated by the fact that hydrostatic pressure enhances intermolecular interactions and changes intramolecular geometry without chemical changes. These experiments were pioneered by Mårdalen *et al.*,[1,2] who reported on the structural and optical transitions for polythiophenes, paving the way for polythiophene studies with fullerene derivatives.[3] These studies were augmented by structural high pressure studies of polyphenylenes by Heimel *et al*[4] and Gitsas *et al*.,[5] and by optical high pressure studies including studies of poly(*p*-phenylene vinylene) by Morandi *et al.*[6] and investigations of fluorene copolymers by Schmidtke *et al.*[7,8] Common to all these studies are planarization of otherwise twisted polymers followed by a redshift in photoluminescence (PL). Also, there are structural high pressure studies of oligoacenes[9] and related molecules including fluorene[10] as well as of related hairy rod type polymers like polyimides,[11-13] which show diverse structural transitions and dependencies between the effect of pressure and side chain structure.

Poly[9,9-bis(2-ethylhexyl)-fluorene-2,7-diyl] (PF2/6)[14] is a stiff conjugated polymer that exhibits 5-[15,16] or 21-helical backbone[17,18] that manifest hexagonal and nematic phases depending on temperature and molecular weight.[19] This polymer is of interest not only because of its optoelectronic properties but also because it represents a model system for other polymer classes including liquid crystalline polymers and hairy rod type polymers. Guha and co-workers studied helical PF2/6 with increasing pressure and observed a redshift in PL concomitant with the significant changes in the Raman spectra.[20] Using X-ray scattering and neon as a pressure transmitting medium, we have subsequently shown that the reported optical changes are concomitant with the reduced order and partial planarization of PF2/6 backbone.[21] With a μm sized X-ray beam, we have also mapped the sample and provided an idea how these effects are spatially distributed above the solidification pressure of neon.[22]

Emergence of non-hydrostatic conditions have been comprehensively described by Klotz *et al.*[23]. The 4:1 mixture of methanol and ethanol shows the glass transition at 10.5 GPa becoming non-hydrostatic. In contrast, neon solidifies at 4.8 GPa but does not become non-hydrostatic until at 15 GPa. This means that neon provides hydrostatic conditions up to higher pressures and was therefore selected as pressure medium in our previous paper.[21] On the other hand, the scattering intensity from polymers is weak and the signal-to-noise ratio low. As an alcohol mixture contains predominantly carbon and oxygen with much fewer electrons than noble gases such as neon, it provides lower scattering background and promises to improve the quality of data by an improved signal-to-noise ratio. This motivates us to replace neon by an alcohol mixture in our current work.

PF2/6 shows a glass transition at about 80 ^{o}C and a transition from hexagonal to nematic phase between 140 ^{o}C and 180 ^{o}C, depending on the molecular weight.[19] Our previous high pressure experiments were performed at room temperature where PF2/6 was expected to be in a deep glassy state.[21,22] As evidenced by the peak width of the Bragg reflections, the data point to reduced structural order not characteristic to the ambient hexagonal structure and the phase behavior remains unclear. Elsewhere, albeit in the MPa pressure regime, Wegner and co-workers[5] studied a related polyphenylene (PPP) type polymer and have shown that the temperatures for phase transitions were increased with increasing pressure. This observation motivates us to conduct high pressure experiment at elevated temperatures.

In this work we repeat earlier measurements at room temperatures replacing neon by an alcohol mixture as a pressure transmitting medium which has potentially for lower scattering background. Furthermore, while the earlier data concern room temperature, we here report on a temperature scan at an elevated pressure. In addition, we compare these results with ambient pressure temperature-

dependent Raman scattering data. We show an accurate mapping from 0.3 GPa to 26 GPa and find a phase transition upon heating.

EXPERIMENTAL

The synthesis of PF2/6 has been described elsewhere.[14] The number- and weight-averaged molecular weights were 95 kg/mol and 188 kg/mol for the polymer used in X-ray scattering measurements and 83 kg/mol and 162 kg/mol for the one used in Raman measurements.

X-ray scattering experiments at elevated pressures were carried out at the Extreme Conditions Beamline (ECB) P02.2 at PETRA III in Hamburg.[24] The X-ray energy was 25.5 keV and the beam size 4 µm × 9 µm (vert. × hor). The sample to detector distance was 88.3 cm. The data were collected by a PerkinElmer XRD 1621 flat panel detector. The *q*-range was calibrated using a CeO_2 standard. Pressure was generated in a diamond anvil cell (DAC) using diamonds with the culet size of 0.3 mm. The DAC consisted of a regular diamond upstream and a perforated diamond downstream reducing Compton scattering background.[25] The DAC was equipped with an intended Rhenium gasket with the 0.15 mm holes. The thickness was reduced from 0.04 mm to 0.02 mm during the experiment. The spatial sample size was about 100 micrometers at the end of the experiment. The 4:1 mixture of methanol-ethanol and neon were used as pressure transmitting media in the first and second experiment, respectively. The polymer sample and the alcohol mixture were introduced manually. Neon was loaded at 1.14 GPa using a gas loader provided by Sanchez Technology and closed at about 1 GPa. The samples were not bridging between the anvils. The pressure scale was calibrated by an internal ruby standard.[26] In the latter experiment, the DAC was heated by resistive heating using a heating jacket covering the whole DAC. The temperature was measured continuously and the sample was left to stabilize 15 minutes in between measurements. The average heating rate was 1 °C/min. The

scattering from an empty DAC was also measured and used for background correction. The sample positioning was based on the scan over the gasket hole. The data treatment followed the one described in Ref.[21]

The Raman spectra were collected by an Invia Renishaw spectrometer attached to a confocal microscope with a 50× long objective and a 785 nm line as the excitation wavelength. The scattered light was collected in a backscattering geometry through a set of optimally aligned edge filters. The samples were affixed to a stainless steel sample holder of a Linkam LTS350 microscope hot-cold stage for temperature dependent studies in the range of -50 °C to 200 °C.

RESULTS AND DISCUSSION

Figure 1(a) plots scattering patterns of PF2/6 in 4:1 mixture of methanol and ethanol with increasing pressure for $q = 0.7 - 0.9$ Å^{-1}. Akin our previous report,[21] the data are dominated by single X-ray reflection which is interpreted as 00*l* reflection that corresponds to the ambient 005 (or 0021) reflection. Figure 1(b) plots the peak position and peak width deduced from the fits of the diffraction (scattering) peak. The peak moves gradually towards higher scattering angle from about 4 GPa upwards. This is concomitant with the optical changes observed by Martin *et al.*,[20] where abrupt shifts in the PL and asymmetry in the Raman line shapes are observed between 2- 4 GPa. Note that the molecular weight of the present polymer corresponds to that used in the paper of Martin *et al.*[20]

The data shown in Fig. 1 are collected from the same sample position. At the same time, the highest pressures clearly exceed the non-hydrostatic limit of the employed alcohol mixture and this means that the actual pressure may vary spatially over the sample. In order to probe this variation, we have previously mapped the ≈ 100 μm sized sample in neon by a less than 10 μm sized X-ray beam.[22]

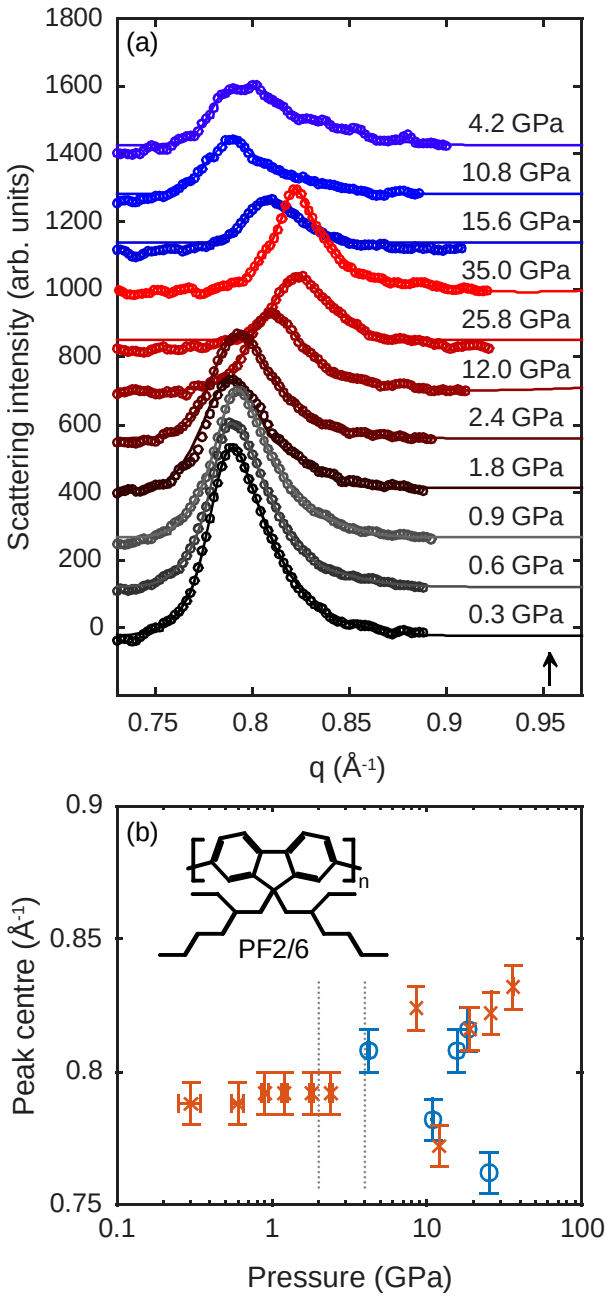

FIGURE 1 (a) Scattering curves (symbols) and fits to the data (solid lines) of PF2/6 with increasing and decreasing pressures. An arrow shows the direction of process. (b) Peak positions obtained from the fits to the observed 00*l* reflection against pressure at room temperature with increasing (red crosses) and subsequently decreasing pressure (blue circles). Dashed lines mark the position of the optical changes reported by Martin *et al*.[20] Inset shows the chemical structure of PF2/6.

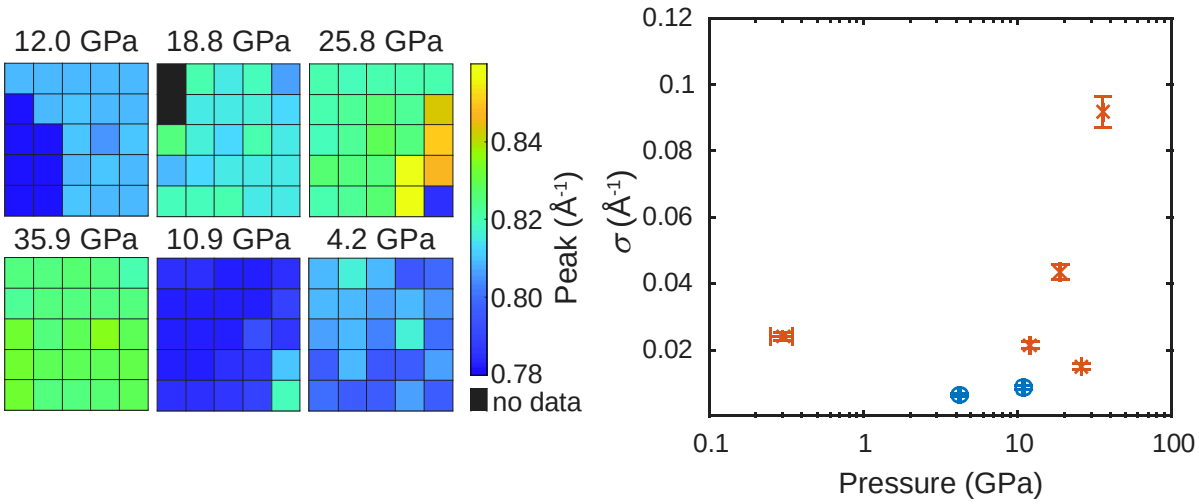

FIGURE 2 Left: Selected subsequent spatial maps of peak positions for the strongest 00*l* reflection for selected pressures over $50\ \mu\text{m} \times 50\ \mu\text{m}$ area with a $10\ \mu\text{m}$ spatial resolution. Right: Corresponding standard deviations calculated to the spatial variation with increased (red crosses) and subsequently decreased pressure (blue circles).

Figure 2 plots spatial maps of 00*l* reflections for selected pressures for PF2/6 in the 4:1 mixture of methanol and ethanol. Each point covers approximately $10\ \mu\text{m} \times 10\ \mu\text{m}$ area and represents similar pressure range shown in Fig. 1. The center is nominally at the same point as the center of the hole (and the sample). Also shown are the spatial averages and the corresponding standard deviations for the fitted peak positions. Our previous consideration indicated smooth shift of the reflection but a sudden jump in its spatial distribution at about 15 GPa, which agrees with the quasi hydrostatic pressure limit of neon.[22] The data shown in Fig. 2 indicates a similar jump at about 10 GPa, in agreement with the quasi hydrostatic pressure limit of the employed alcohol mixture. These considerations show that PF2/6 is sensitive to the non-hydrostatic conditions regardless the pressure transmitting medium and we see a pressure and thus structure gradient. The ideal pressure distribution would be homogeneous and radial from the center. However, our maps do not point to the radial pressure distribution, which may imply asymmetric deformation of the gasket.

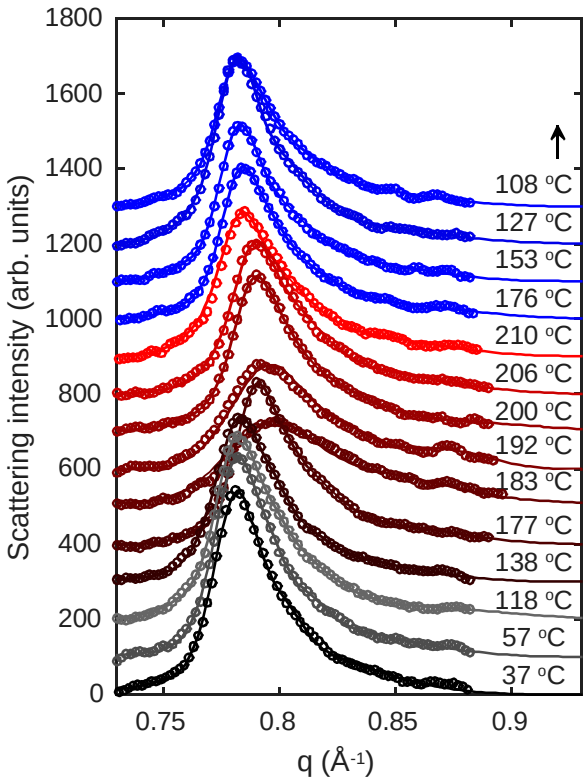

FIGURE 3 Scattering curves (symbols) and fits to the data (solid lines) of PF2/6 as a function of temperature at the constant pressure at 4.3 GPa. An arrow shows the direction of process. The heating rate was 1 ^{o}C/min.

Figure 3 plots the scattering patterns of PF2/6 in neon with increasing temperature at the nominally constant pressure 4.3 GPa. Figure 4 plots the corresponding peak shape analysis. We find that the pressure may vary by 0.1-0.3 GPa upon heating. However, this pressure is still below the solidification of neon and the conditions may be assumed to be quasi hydrostatic. Again, the scattering data are dominated by 00*l* reflection. The curves are seemingly similar but a shift towards higher scattering angles becomes visible at 167 °C upon heating. A reversible shift back is observed at 176 °C upon cooling. This is accompanied by a shift in the peak width; these peak characteristics mimicking the ambient transition from the hexagonal to the nematic phase.[19] This ambient transition for the polymer whose molecular weight matches the here investigated polymer is 164 °C upon heating. If these transitions have the same physical origin, it means the shift towards higher temperatures with increasing pressure is way smaller than the one reported by Gitsas *et al*.[5]

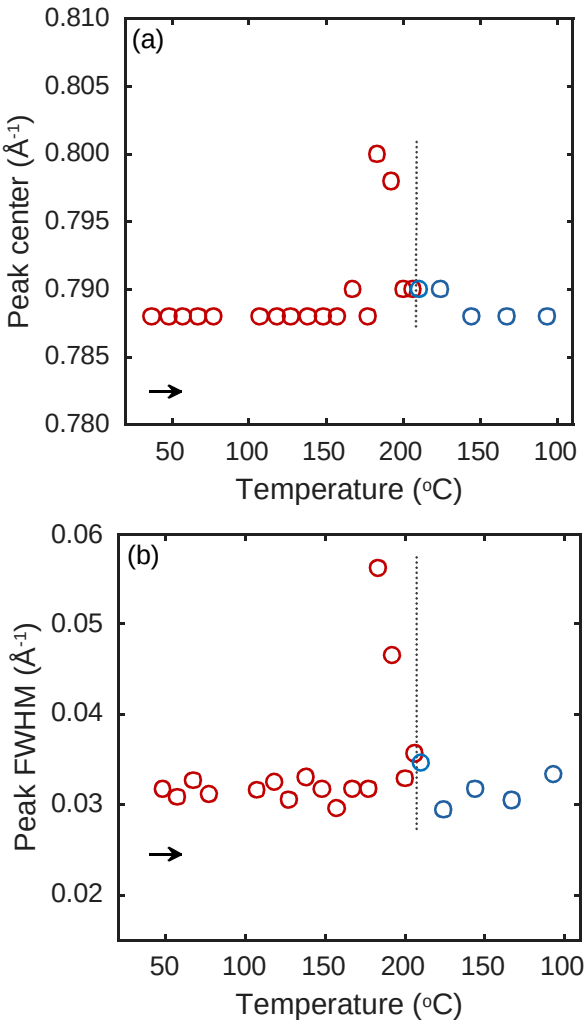

Figure 4 (a) Peak positions and (b) peak width obtained from the fits to the observed 00*l* reflection during a heating-cooling cycle at 4.3 GPa. Increasing temperature is marked by red and decreasing by blue, the turning point marked by vertical dotted lines. Arrows show the direction of process.

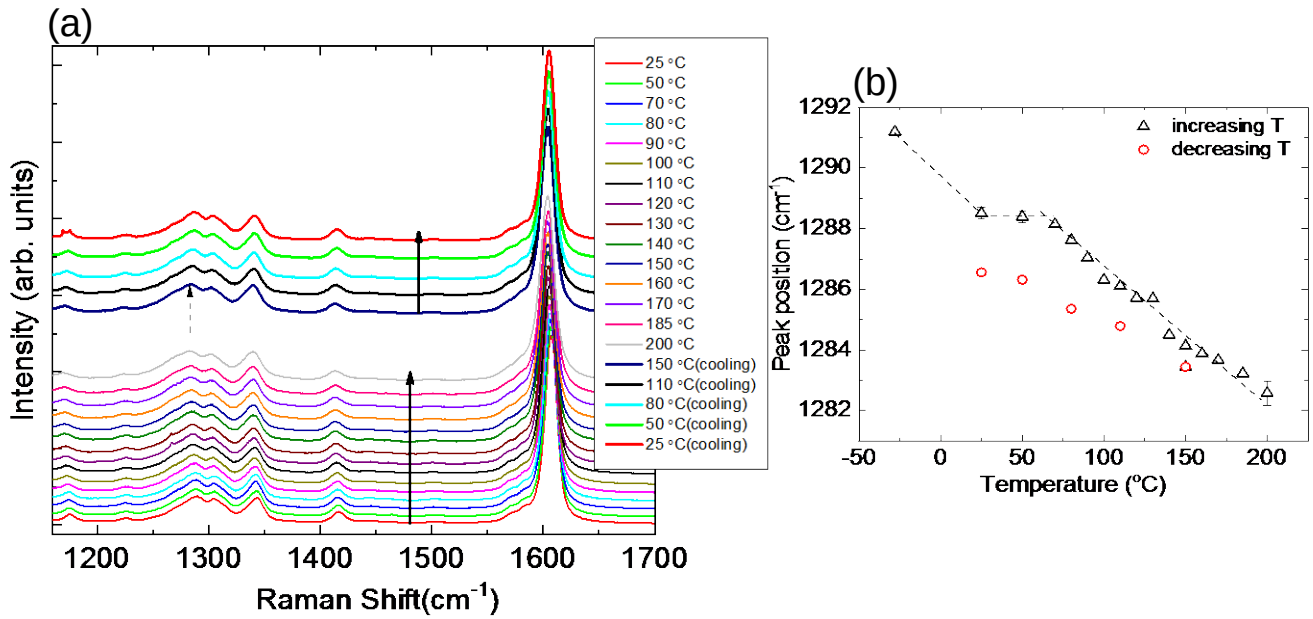

Figure 5 (a) Raman spectra of PF2/6 under ambient pressure and as a function of temperature. The top five spectra were measured upon cooling the sample. The arrows point in the direction of increasing (and decreasing) temperatures. The peak at 1285 cm^{-1} is shown with a dotted line. (b) The peak position of the 1285 cm^{-1} Raman peak shown with increasing and decreasing temperatures.

The temperature dependence of the XRD data of PF2/6 under ambient conditions shows subtleties, especially depending on annealing and cooling times.[16] An extended annealing slightly below the glass transition temperature sharpens and increase the intensity of the 00*l* reflection, suggestive of a cold crystallization due to a high interchain ordering. Upon cooling of the polymer from 160 °C, this long-range ordering is retained. Raman scattering measurements with similar annealing and cooling times were performed and in general, agreed with the X-ray scattering measurements. We repeated these measurements at ambient conditions using a similar molecular wt. sample as was used for high pressure X-ray scattering experiment, and with long annealing times.

For comparisons we show in Figure 5 (a) the Raman spectra in the 1200-1700 cm^{-1} range at various temperatures collected at ambient pressure. For detailed analysis of the Raman peaks in this range, see Ref.[16]. The region between 1250 -1350 cm^{-1} corresponds to the backbone C-C stretch modes. This entire region was fit by Lorentzian peaks. Figure 5(b) plots the 1285 cm^{-1} Raman peak as a function of both increasing and decreasing temperature. Between room temperature and the glass transition temperature of ~ 80 °C, the peak position hardly changes. We see a similar trend for all the Raman peaks in this region. We point out that the annealing times also play a role; in our prior work the Raman peak positions were almost constant until 150 °C.[16] In the data shown here, the sample was held for more than 15 hrs between the glass transition temperature (80 °C) and 90 °C. Upon increasing the temperature to 200 °C, the sample assumes the hexagonal phase and upon cooling to room temperature, this long range order is still preserved.

The Raman data indicates a cold crystallization process between ambient temperature and the glass transition temperature, which is also observed in the X-ray data at 4.2 GPa, although till even higher temperatures of 160 °C. This suggests slightly different kinetics in the crystallization process between ambient conditions and under a pressure of ~ 4 GPa.

CONCLUSIONS

PF2/6 becomes planarized with increased pressure concomitant with the earlier reported optical effects at $2-4\,\mathrm{GPa}$. This effect becomes laterally inhomogeneous for $>10\,\mathrm{GPa}$ attributed to the solidification of pressure transmitting medium. The use of an X-ray microbeam is a way to quantify this variation. PF2/6 shows a phase transition at 167-176 °C at the constant pressure 4.3 GPa in neon. From the above experiments, we suggest using alcohol medium and perforated diamonds to reduce the scattering background. The kinetics of the phase transition seems to be different at ambient pressure versus elevated pressure. The Raman scattering data (frequency position) from PF2/6 as a function of temperature at ambient pressure shows almost no change between room temperature and the glass transition temperature. This work is one step forward in the process revealing the high pressure behavior of polyfluorenes. The forthcoming work includes more comprehensive thermal studies against pressure clarifying the nature of observed thermal transition as well as molecular dynamics simulations incorporating both pressure and temperature. In the future, we will also screen avenues for high pressure polymer chemistry as is already emerging elsewhere.[27,28]

ACKNOWLEDGEMENTS

This research was carried out at the light source PETRA III at DESY, a member of the Helmholtz Association (HGF). We thank DANSCATT for financial support.

REFERENCES

1 J. Mårdalen, Y. Cerenius, P. Häggkvist, *J. Phys.: Condens. Matter* **1995**, *7*, 3501-3506.

2 J. Mårdalen, E. J. Samuelsen, O. R. Konestabo, M. Hanfland, M. Lorenzen, *J. Phys.: Condens. Matter* **1998**, *10*, 7145-7154.

3 Y. Noguchi, A. Saeki, T. Fujiwara, S. Yamanaka, M. Kumano, T. Sakurai, N. Matsuyama, M. Nakano, N. Hirao, Y. Ohishi, S. Seki, *J. Phys. Chem. B* **2015**, *119*, 7219-7230.

4 G. Heimel, P. Puschnig, M. Oehzelt, K. Hummer, B. Koppelhuber-Bitschnau, F. Porsch, C. Ambrosch-Draxl, R. Resel, *J. Phys.: Condens. Matter* **2003**, *15*, 3375-3389.

5 A. Gitsas, G. Floudas, G. Wegner, *Phys. Rev. E* **2004**, *69*, 041802.

6 V. Morandi, M. Galli, F. Marabelli, D. Comoretto, *Phys. Rev. B* **2009**, *79*, 045202.

7 J. P. Schmidtke, J.-S. Kim, J. Gierschner, C. Silva, R. H. Friend, *Phys. Rev. Lett.* **2007**, *99*, 167401.

8 J. P. Schmidtke, R. H. Friend, C. Silva, *Phys. Rev. Lett.* **2008**, *100*, 157401.

9 M. Oehzelt, A. Aichholzer, R. Resel, G. Heimel, E. Venuti, R. G. Della Valle, *Phys. Rev. B* **2006**, *74*, 104103.

10 G. Heimel, K. Hummer, C. Ambrosch-Draxl, W. Chunwachirasiri, M. J. Winokur, M. Hanfland, M. Oehzelt, A. Aichholzer, R. Resel, *Phys. Rev. B* **2006**, *73*, 024109.

11 K. Takizawa, H. Fukudome, Y. Kozaki, S. Ando, *Macromolecules* **2014**, *47*, 3951-3958.

12 K. Takizawa, J. Wakita, S. Azami, S. Ando, *Macromolecules* **2011**, *44*, 349-359.

13 E. Fujiwara, H. Fukudome, K. Takizawa, R. Ishige, S. Ando, *J. Phys. Chem. B* **2018**, *122*, 8985-8997.

14 M. Grell, W. Knoll, D. Lupo, A. Meisel, T. Miteva, D. Neher, H.-G. Nothofer, U. Scherf, A. Yasuda, *Adv. Mater.* **1999**, *11*, 671-675.

15 G. Lieser, M. Oda, T. Miteva, A. Meisel, H.-G. Nothofer, U. Scherf, D. Neher, *Macromolecules* **2000**, *33*, 4490-4495.

16 B. Tanto, S. Guha, C. M. Martin, U. Scherf, M. J. Winokur, *Macromolecules* **2004**, *37*, 9438-9448.

17 M. Knaapila, M. Torkkeli, A. P. Monkman, *Macromolecules* **2007**, *40*, 3610-3614.

18 M. Brinkmann, N. Charoenthai, R. Traiphol, P. Piyakulawat, J. Wlosnewski, U. Asawapirom, *Macromolecules* **2009**, *42*, 8298-8306.

19 M. Knaapila, R. Stepanyan, M. Torkkeli, B. P. Lyons, T. P. Ikonen, L. Almásy, J. P. Foreman, R. Serimaa, R. Güntner, U. Scherf, A. P. Monkman, *Phys. Rev. E* **2005**, *71*, 041802.

20 C. M. Martin, S. Guha, M. Chandrasekhar, H. R. Chandrasekhar, R. Guentner, P. Scanduicci de Freitas, U. Scherf, *Phys. Rev. B* **2003**, *68*, 115203.

21 M. Knaapila, Z. Konôpková, M. Torkkeli, D. Haase, H.-P. Liermann, S. Guha, U. Scherf, *Phys. Rev. E* **2013**, *87*, 022602.

22 M. Knaapila, M. Torkkeli, Z. Konôpková, D. Haase, H.-P. Liermann, U. Scherf, S. Guha, *Macromolecules* **2013**, *46*, 8284-8288.

23 S. Klotz, J.-C. Chervin, P. Munsch, G. Le Marchand, *J. Phys. D: Appl. Phys.* **2009**, *42*, 075413.

24 H.-P. Liermann, Z. Konôpková, W. Morgenroth, K. Glazyrin, J. Bednarcik, E. E. McBride, S. Petitgirald, J. T. Delitz, M. Wendt, Y. Bican, A. Ehnes, I. Schwark, A. Rothkirch, M. Tischer, J. Heuer, H. Schulte-Schrepping, T. Kracht, H. Franz, *J. Synchrot. Rad.* **2015**, *22*, 908-924.

25 E. Soignard, C. J. Benmore, J. L. Yarger, *Rev. Sci. Instrum.* **2010**, *81*, 035110.

26 P. M. Bell, H. K. Mao, K. Goettel, *Science* **1984**, *226*, 542-544.

27 L. Qiu, M. Peña-Alvarez, M. Taravillo, P. J. Evans, E. R. Darzi, R. Jasti, P. M. Burrezo, J. T. L. Navarrete, V. G. Baonza, J. Casado, M. Kertesz, *Chem. Eur. J.* **2017**, *23*, 16593-16604.

28 L. Qiu, M. Pena-Alvarez, V. G. Baonza, M. Taravillo, J. Casado, M. Kertesz, *ChemPhysChem* **2018**, *19*, 1903-1916.